

Analytical and Numerical Investigation of Significant Parameters on Strength of Electromagnetically Assembled Aluminum Tube Joints

Mehdi Zohoor^{1*}, Bahman Ghorbani²

¹Associate professor, Faculty of Mechanical Engineering, K.N.T Uni. of Tech., Tehran, Iran

*Email of Corresponding Author: mehdizohoor@gmail.com

²MSc. in Mechanical Engineering, K.N.T Uni. of Tech., Tehran, Iran

Received: 30 April, 2014; Accepted: 5 July, 2014

Abstract

Electromagnetic forming is a high energy rate forming process in which an electromagnetic Lorentz body force is used for deformation of products. In this article, electromagnetic forming process was simulated for the assembly of parts as an innovative method. The effect of important process parameters such as discharge energy, radius and width of rectangular groove on the strength of the assembled products were studied by using finite element technique and design of experiment. After introducing the governing equations, the output of these equations were applied in simulation as a pressure on work-piece. In this simulation, an ax symmetric model was used in analysis and Johnson-Cook theory was applied due to high strain rate to show the plastic behavior of the materials. Finally, the numerical results were compared with the experimental ones reported by other researchers and a good correlation was found between them. Results revealed that the bead depth increases with the increase of the discharge energy and more filling groove, increasing strength of joint. Also Strength of joint increases due to the creation of partial shearing of the tube at the groove edge and interference stresses at the tube and mandrel interface.

Keywords

Electromagnetic forming, Finite element, Groove, Aluminum tube, Strength of joint.

1. Introduction

One of the most attractive high-speed forming methods is electromagnetic forming [1], which uses Lorentz forces to form metals with high electrical conductivity, such as aluminum alloys, magnesium, copper, silver, brass, and steel [2].

This method is used for forming and joining metals together. The main application of this process is in automotive industries, aerospace, especially in parts assembly [3, 4].

Economical production of high strength joints is a major challenge to produce the vehicle structure. The automotive industry applies this process to reduce the weight of the cartooptimize power train (Fig. 1).

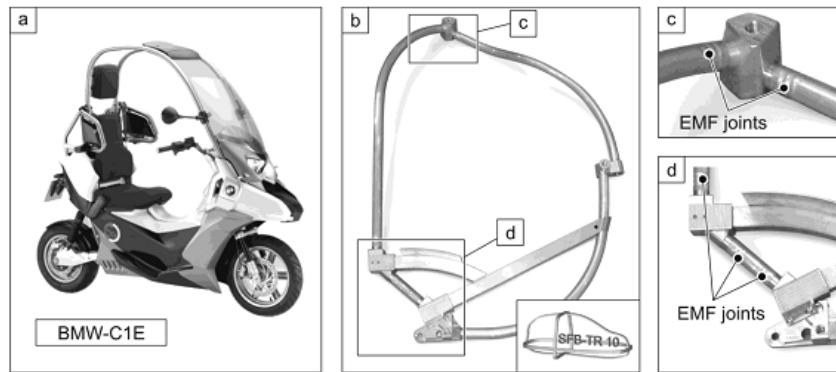


Fig.1.a) BMW-C1E. b) Alternative frame structure for the BMW-C1E manufactured with in the collaborative research center SFB/TR10. c) and d) EMF form-fit joints [5]

Electromagnetic joining of tubular work-pieces can be classified into three main categories, according to the dominant mechanism [6,7]:

1. Interference fits: the outer element (tube) undergoes plastic deformation and the internal part (mandrel) deforms in a purely elastic manner. After the completion of the forming and the decrease of the forces, the internal part tends to return to its original shape (elastic relaxation), but is being restrained by the plastically deformed tube. As a result, interference stresses are generated between both joining partners.
2. Form fits: an undercut (e.g. a groove) is applied in the internal part and the other element (tube) is deformed into this undercut, thus creating mechanical interlock.
3. Welded joints: are attached on a micro-structural level.

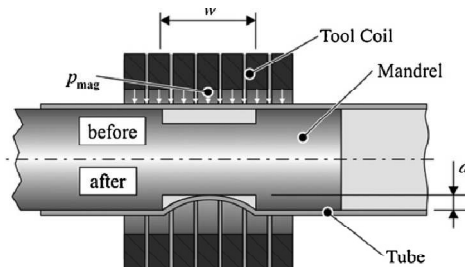


Fig.2.Schematic of the form fit by EMF for a mandrel with a rectangular groove (before and after deformation) [5]

To determine the best shape of the groove in the internal part, three options were investigated in detail in literature: triangular, circular and rectangular grooves.

Joints with triangular grooves are always the weakest. This is because for triangular grooves the angle α is greater than for rectangular or circular grooves. This results in a lower degree of deformation at the groove edge, and thus a smaller tensile force is required to initiate the pull-out of the tube from the groove [6,7].

The circular grooves have a smaller resulting angle α than the rectangular, but the rectangular grooves still have a larger pull-out force because of the larger amount of shearing of the tube into the rectangular groove. This better locks the tube in place. Joints formed with rectangular grooves will always exhibit the highest joint strength.

The strength of the rectangular groove of form fits strongly depends on three factors which determine the groove geometry: its depth and width and the radius at the groove edges (Figure 3).

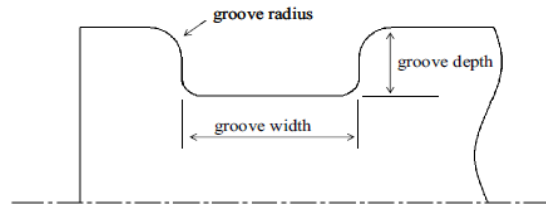


Fig.3.The geometric parameters of the groove [8]

Bühler, Golovashchenko [7], and Park [8] studied the effect of various parameters on the strength of form fit joints.

Bühler and Golovashchenko investigated the effect of groove width and depth on the strength of form fit joints, by using electromagnetic pressure.

In their study, they use different pressures, so that only tube wall touched the groove bottom. They found that increasing the width and depth of the groove provides a stronger joint.

Compared with Bühler and Golovashchenko, Park used constant pressure and found an increase in the strength of joint with increasing depth and width of the groove.

There is a limit of the joint strength when a single groove is used, even though the groove configuration is optimized. In other words, a single groove does not produce full strength of the material. This is because thinning after EMF cannot be avoided. Thus, two or more grooves must be used to obtain full strength of the material. But, it is meaningless to increase two or more grooves with the same configuration because the joint strength is not made arithmetically. In other words, combining two units of the groove which have 50% joint strength does not yield 100% joint strength. This behavior is due to stress concentration at the end of the tube caused by the differential strain of the outer member [8].

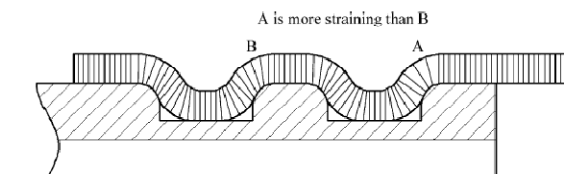


Fig.4. Schematic explanation of the differential strain [8]

When a tensile load is exerted on joined tubes, the inner steel tube will move as a rigid body and the outer aluminum tube will suffer deformation. Each tube bears the full load just before the joint and transmits it gradually to the other. Thus the stress of outer aluminum tube will be highest at A and gradually diminish toward B. On the contrary, the stress of the inner steel tube will be highest at B and diminish toward A. As the outer aluminum tube is extensible and the inner steel tube is inextensible, only the outer member will develop strains proportional to the existing stresses and failure will occur around A. In this paper, we shall count the groove from A to B. The first groove means the groove close to the end of the inner tube.

Joints which have less thinning toward the first groove are stronger than the others. This is due to the stress concentration at the edge of the joint as mentioned above.

To produce full strength of the material, groove configuration should satisfy the following conditions:

- Thickness reduction on the first groove is minimized or removed because material thickness on the first groove mainly governs the joint strength.
- The joint should be designed to reduce thinning toward the first groove. The groove depth should be shallower.

AL 1100 has wide application in automotive industry. Accordingly, we used a tube AL 1100 with inner diameter of 47 mm and thickness of 0.6 mm.

In this paper, the effect of some important parameters, such as discharge energy, radius, and width of the groove were investigated by using the ABAQUS finite element software and design of experiments.

For this purpose, both factors, i.e. radial displacement and thinning, have important role on strength joint.

Therefore, these two factors are considered as output variables and factors (discharge energy, radius and width of the groove) as input variables have been considered.

After designing experiments, process simulations were carried out according to the output variables (radial displacement and thinning) measurements and then using ANOVA, the effect of input variable on the output was investigated.

The advantage of this method is that it is possible to investigate the interaction of effects and to minimize the number of tests required.

2. Assumptions

Due to the complex physical nature of this process, it is intended to be simplified by the following assumptions:

1. During electromagnetic forming process, the work-piece within a few microseconds reaches to a high speed and moves away from the coil. In this case, the electromagnetic field changes due to changing mutual inductance between the coils and the work-piece. The interaction between the work-piece movement and the density of the magnetic field is negligible and it is assumed that the magnetic field has no effect on sheet speed.
2. Since the electromagnetic forming process occurs in a very short time, so the inductance is assumed to be constant during the forming process.
3. Because of symmetry, an axi-symmetrical configuration is used for the work-piece and coil during numerical simulation. As a result, the magnetic field and the electromagnetic force acts on the surrounding of the tube do not change.
4. Electromagnetic properties are assumed constant and heat effects are not considered.

3. Electromagnetic equations

Using the quasi-static Maxwell's equations for a cylindrical coordinate system, the density of the magnetic field B , with two components radial B_r and axial B_z is obtained as follows [9]:

$$-\frac{1}{\mu_0 \sigma_w} \left(\frac{\partial^2}{\partial r^2} + \frac{1}{r} \frac{\partial}{\partial r} + \frac{\partial^2}{\partial z^2} - \frac{1}{r^2} \right) B_r + \frac{\partial B_r}{\partial t} = 0 \quad (1)$$

$$-\frac{1}{\mu_0 \sigma_w} \left(\frac{\partial^2}{\partial r^2} + \frac{1}{r} \frac{\partial}{\partial r} + \frac{\partial^2}{\partial z^2} \right) B_z + \frac{\partial B_z}{\partial t} = 0 \quad (2)$$

μ_0 is the permeability of free space, σ is electrical conductivity of the work-piece and t is time. Assuming ax symmetric, eddy current only has surrounding component, which is defined as follows:

$$j_\theta = \frac{1}{\mu_0} \left(\frac{\partial B_r}{\partial z} - \frac{\partial B_z}{\partial r} \right) \quad (3)$$

Lorentz force has radial and axial components, which include:

$$f_r = j_\theta B_z \quad (4)$$

$$f_z = -j_\theta B_r \quad (5)$$

Radial and axial of electromagnetic pressure by using integral are calculated as follows:

$$P_r = \int_{z=0}^{z=hw} f_r dr \quad (6)$$

$$P_z = \int_{z=0}^{z=hw} f_z dr \quad (7)$$

Where hw is tube wall thickness.

4. Simulation algorithm

In simulation of the electromagnetic forming, there is an interaction between electromagnetic force and the work-piece during the forming process. In other words, there is coupling between electromagnetic field and specimen for each small time interval.

There are two algorithms, loose-coupled and sequential-coupled algorithm for electromagnetic forming simulation [10-13].

In the loose-coupled method, the equations governed electromagnetic parts of the problem are assumed independent of the structural part of it.

But in the sequential-coupled algorithm, electromagnetic and structure-mechanical simulations are iteratively and sequentially performed and changing the work-piece geometry is a function of time and it is considered in solving governing equations in the electromagnetic part.

The method used in this research is that electromagnetic equations code was written in FORTRAN.

It was performed in subroutine to compute the applied electromagnetic pressure.

The pressure is applied on each single node of tube at any period and on mechanical part that leads to deformation of the work-piece. This computation was performed at each time step.

5. Finite element Simulation

ABAQUS finite element software was used for simulation. The model involves die and tube that are modeled 2D (plane strain) because of axi-symmetry. In this simulation, work-piece was modeled deformable wire element with an axisymmetric model in ABAQUS and seeded 50 meshes SAX1 along tube length. The die (mandrel) was assumed rigid.

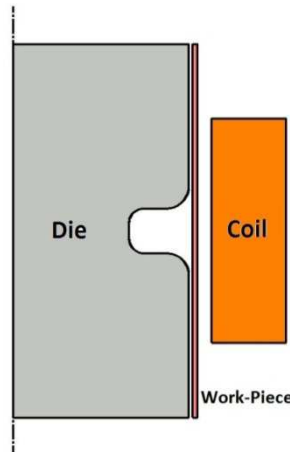


Fig.5.Schematic of tube compressive process including work-piece, coil and die in ax symmetric

Subroutine was used for applying pressure in simulation. Same as ref. [14], temperature rising was neglected due to the induced current, and simulation process time was fixed at 35 μs [3]. Using time step to stable simulation process took 0.1 μs.

The Johnson-Cook theory was applied due to high strain rate to show the plastic behavior of the materials [15].

$$\bar{\sigma} = [A + B\bar{\epsilon}^n] \left[1 + C \ln \left(\frac{\dot{\bar{\epsilon}}}{\dot{\bar{\epsilon}}_0} \right) \right] \left[1 - \left(\frac{T - T_r}{T_m - T_r} \right)^m \right] \quad (8)$$

Where,

$\bar{\sigma}$ =Flow stress

A=Yield stress

B=Coefficient of strain hardening

n=Strain hardening exponent

c=Sensitivity coefficient to strain rate

$\dot{\bar{\epsilon}}$ =Plastic strain rate of the work-piece at moment time

$\dot{\bar{\epsilon}}_0$ =Reference plastic strain rate

T=Work-piece temperature

T_m =Melting point of the material

T_r =Transition temperature

m=Material coefficient that is softening of the material at high temperature

Johnson-Cook constants, mechanical and physical properties are listed in tables (1) and (2):

Table1.Johnson-Cook coefficients for AL1100-H12 tube[16]

| A(Mpa) | B(Mpa) | C | m | n | $\dot{\bar{\epsilon}}_0$ |
|---------|---------|-------|-------|-------|--------------------------|
| 148.361 | 345.513 | 0.001 | 0.859 | 0.183 | 1 |

Table2. Mechanical and physical properties of AL1100-H12 tube[16]

| | | | | | |
|-----------------|----------------------|------------------------|----------------------|-----------------|--------------------------|
| Density (Kgm-3) | Yield Strength (MPa) | UltimateStrength (MPa) | Young'sModulus (GPa) | Poisson's ratio | Melting Temperature (°C) |
| 2700 | 148.361 | 345.513 | 65.762 | 0.3 | 620 |

In this simulation, work-piece was modeled deformable wire element with an axisymmetric model in ABAQUS and seeded 50 meshes SAX1 along the tube length and coulomb coefficient friction was assumed to be 0.15.

6. Design of experiment

Several parameters influence the final strength joint that was assembled by electromagnetic forming. Discharge energy, radius and width of the groove on radial displacement and the work-piece thinning. So they are considered as responses.

To determine them aximumthinning on wall thickness of the tube, equation (9) is used.

$$\% \text{ Thinning} = \frac{t_0 - t_f}{t_0} \times 100 \tag{9}$$

t0 is the initial wall thickness of the tube, and tf is the final wall thickness of the tube.

Table3.parameters with their levels

| Parameters | | Low level | Mid. level | High level |
|------------------|-----|-----------|------------|------------|
| Discharge energy | (A) | 2.4 | - | 3.6 |
| Width of groove | (B) | 3 | 6 | 9 |
| Radius of groove | (C) | 3 | 4.5 | 6 |

According to the full factorial method, there exist 18 possible tests for measured design [17].

Table4: Test matrix with simulation results

| No. | Discharge energy [mm] | Width of groove [mm] | Radius of groove [mm] | Radial displacement [mm] | Thinning [%] |
|-----|-----------------------|----------------------|-----------------------|--------------------------|--------------|
| 1 | 2.4 | 3 | 3 | 2.077 | 2.583 |
| 2 | 2.4 | 3 | 4.5 | 2.609 | 2.633 |
| 3 | 2.4 | 3 | 6 | 2.877 | 1.950 |
| 4 | 2.4 | 6 | 3 | 2.714 | 2.850 |
| 5 | 2.4 | 6 | 4.5 | 2.893 | 2.116 |
| 6 | 2.4 | 6 | 6 | 2.948 | 0.750 |
| 7 | 2.4 | 9 | 3 | 2.905 | 2.116 |
| 8 | 2.4 | 9 | 4.5 | 2.949 | 0.650 |
| 9 | 2.4 | 9 | 6 | 2.963 | 0.133 |
| 10 | 3.6 | 3 | 3 | 2.61 | 3.416 |
| 11 | 3.6 | 3 | 4.5 | 3.247 | 3.8 |
| 12 | 3.6 | 3 | 6 | 3.768 | 3.25 |
| 13 | 3.6 | 6 | 3 | 3.52 | 4.5 |
| 14 | 3.6 | 6 | 4.5 | 3.906 | 3.683 |
| 15 | 3.6 | 6 | 6 | 4.066 | 2.116 |
| 16 | 3.6 | 9 | 3 | 3.955 | 3.716 |
| 17 | 3.6 | 9 | 4.5 | 4.082 | 2.083 |
| 18 | 3.6 | 9 | 6 | 4.123 | 0.55 |

7. Results and Discussion

Maximum thinning occurs on contact radius of the groove due to the occurrence of tensile stresses (Figure6).

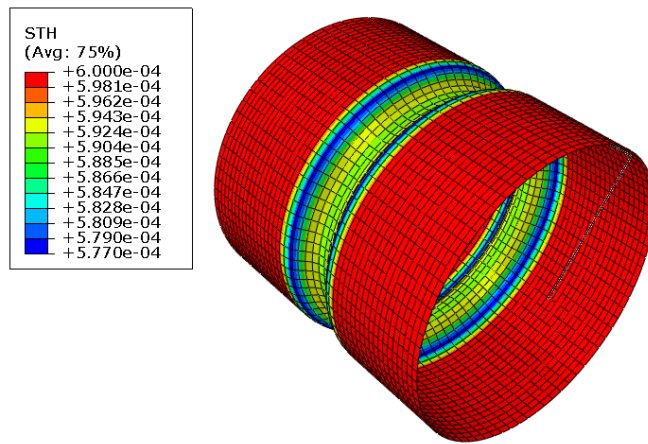


Fig.6.Thickness distribution along the length of the tube

Smaller radius of the groove causes stress concentration and creating partial shearing of the tube at the groove edge and larger radius causes the tube to be removed easily from the Mandrel during the pull-out test.

Groove radius should be specified so that the thickness reduction and separation of the joint can be prevented. This means that the optimum groove radius depends on the thickness of the tube.

7.1 Discharge energy

Increasing discharge energy leads to increasing the magnetic field density and magnetic pressure, as a result, increasing radial displacement of tube wall thickness into groove, which agrees with Ref. [3].

The increase in the charging energy meant that the groove was more filled than the defined condition for just “filling,” which was the first point where the tube made contact with the bottom surface of the groove. With an increase in the charging energy, more of the tube surface was in contact with the bottom of the groove, as shown in Fig. 7.

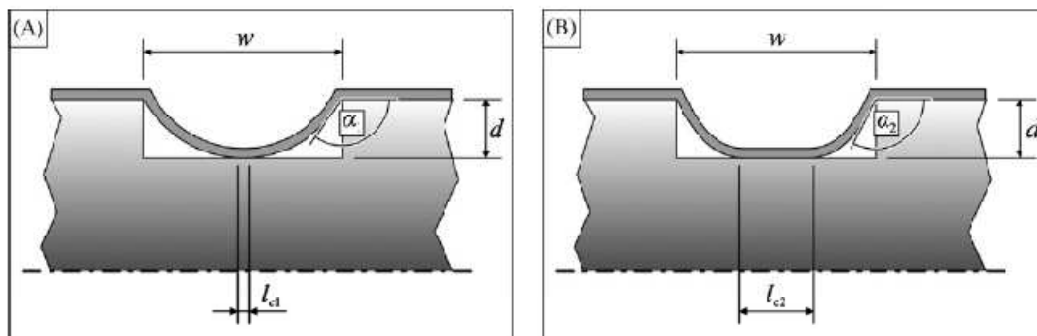


Fig.7.(A) A joint manufactured with a minimal necessary charging energy to fill the groove. (B) A joint manufactured with a higher charging energy [5]

This results in the interference stresses at the contact surface between the tube and mandrel. This interference stress will resist the tube pull-out during tensile testing, thereby increasing joint strength.

Another reason for increasing the joint strength with increase in the charging energy is the decrease of the resulting angle α of the tube wall at the edge of the groove. The decrease in the resulting angle that occurs with an increase in the charging energy means that there is a higher degree of deformation at the groove edge, which requires a higher pull-out force to cause failure. Thus, joint strength is increased.

7.2 Effect of the groove width and radius

An increasing in the width of the groove radius leads to an increase in the bending moment on the sheet and thus the radial displacement increases.

However, as shown in Figure8, with increasing the width of the groove, the groove radius has very little or no effect. In other words, the effect of groove width is much greater than the radius of the groove.

By increasing the width of the groove, the groove bottom creates more surface area which leads to a greater interaction and joint streng this stronger.

But there is a limitation, because the increase in the track width causes wrinkles is greater than a specified point and because the increasing weight of the product and the cost of materials is not economically viable.

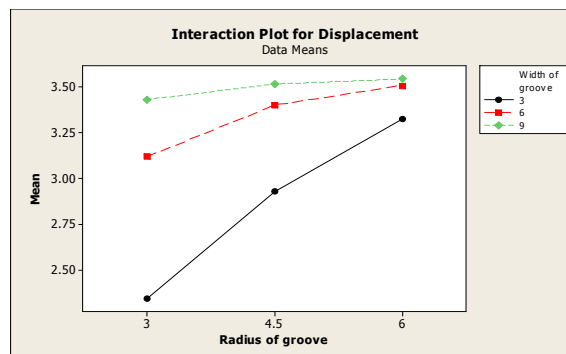


Fig.8. Interactions of parameters effective on radial displacement

8. Conclusion

Aluminum tubes form-fit by electromagnetic forming, which is a new approach for manufacturing light weight automotive structure, was performed by using finite element method and the effects of some important parameters were investigated on radial displacement and thinning of the work-pieces and the following conclusions were extracted from the results:

Increasing the discharge energy leads to increasing the magnetic field density and magnetic pressure, as a result, increasing the radial displacement of tube wall thickness into groove. With a constant groove depth, increasing the discharge energy leads to increasing filling and consequently stronger strength joint.

Creating partial shearing of the tube at the groove edge leads to mechanical lock and also increasing the strength of joint.

Interference stresses at the tube and mandrel interface lead to increasing the strength of joint and is recommended for increasing interference fit, knurling mandrel surface.

9. Symbols

| symbols | Description |
|------------|-----------------------------------|
| B_r | Radial magnetic field density |
| B_z | Axial magnetic field density |
| f_r | Radial Lorentz force |
| f_z | Axial Lorentz force |
| h_w | Tube wall thickness |
| t | time |
| t_0 | Initial tube wall thickness |
| t_f | Final tube wall thickness |
| P_r | Radial electromagnetic pressure |
| P_z | Axial electromagnetic pressure |
| μ_0 | Permeability |
| σ_w | Electrical conductivity workpiece |
| J_θ | Surrounding eddy current |

10. References

- [1] Ghorbani, B., 2014, Investigation of electromagnetic forming parameters for manufacturing metal parts by using finite element method, MSc Thesis, Faculty of Mechanical Engineering, K.N.Toosi University of Technology.
- [2] Sedighi, M., Karimi-nemch, H., Khandai, M. 2012. "Effect of sheet thickness on magnitude and distribution of magnetic force in electromagnetic sheet metal forming process", Applied mechanics and materials, Vol.110-116, 3506-3511.
- [3] FallahiArezoodar, A.R., Ebrahimi, H. and Farzin, M. 2012. Numerical and Experimental Investigation of Inward Tube Electromagnetic forming-Electromagnetic Study. Advanced Materials Research, 383(390), 6710-6716.
- [4] El-Azab, A., Garnich, M. and Kapoor, A. 2003. "Modeling of the electromagnetic forming of sheet metals: state-of-the-art and future needs". Journal of Materials Processing Technology, 142, 744-754.
- [5] Weddeling, C., Woodward, S., Nellesen, J., Psyk, V., Marré, M., Brosius, A., Tekkaya, A.E., Daehn, G.S., Tillmann, W. 2010. "Development of design principles for form-fit joints in lightweight frame structures", 4th International Conference on High Speed Forming.
- [6] Wonterghem, M.V. and Vanhulsel, P. 2011. Magnetic pulse crimping of mechanical joints, MSc. thesis, Gent University, Belgium.
- [7] Weddeling, C., Woodward, S. T., Marré, M., Nellesen, J., Psyk, V., Tekkaya, A.E. and Tillmann, W. 2011. Influence of groove characteristics on strength of form-fit joints, Journal of Materials Processing Technology, 211, 925-935.
- [8] Park, Y.B., Kim, H.Y. and Oh, S.I. 2005. Design of axial/torque joint made by electromagnetic forming. Journal of Thin-Walled Structures, 43, 826-844.
- [9] Siddiqui, M.A. 2009. Numerical Modeling and simulation of electromagnetic Forming process, Ph.D. thesis, Strasbourg University.
- [10] Bartels, G., Schätzing, W., Scheibe, H.P. and Leone, M. 2009. Comparison of two different simulation algorithms for the electromagnetic tube compression, International Journal of Mater Form, 2(1), 693-696.
- [11] Pérez, I., Aranguren, I., González, B. and Eguial, I. 2009. Electromagnetic forming: A new coupling method. International Journal of Mater Form, 2(1), 637-640.

- [12] Haiping, Y.U., Chunfeng, L.I. and Jianghua, D.E.N.G. 2009. Sequential coupling simulation for electromagnetic–mechanical tube compression by finite element analysis, *journal of materials processing technology*, 209, 707–713.
- [13] Bartels, G., Schätzing, W., Scheibe, H.P. and Leone, M. 2008. Models for Electromagnetic Metal Forming, 3rd International Conference on High Speed Forming.
- [14] Jablonski, J. and Wrinkler, R. 1978. Analysis of the electromagnetic forming process, *International Journal of mechanical sciences*, 20, 315–25.
- [15] Johnson, G. R. and Cook, W. H. 1983. A constitutive model and data for metal subjected to large strains, high strain rates and high temperatures, *The Netherlands Proceeding seventh International Symposium on ballistic*.
- [16] Gupta, N.K. ,Iqbal, M.A. and Sekhon, G.S. 2006. Experimental and numerical studies on the behavior of thin aluminum plates subjected to impact by blunt- and hemispherical-nosed projectiles. *International Journal of Impact Engineering*, 32, 1921–1944.
- [17] Montgomery, D.C. 2001. *Design and Analysis of Experiments*.5th Edition, John Wiley & SonsInc, New York.

